FOI-R--1320--SE
September 2004
1650-1942

Scientific report

Stephen Conway

Implementation and Validation of an Engine Nacelle Boundary Condition in Edge 3.2

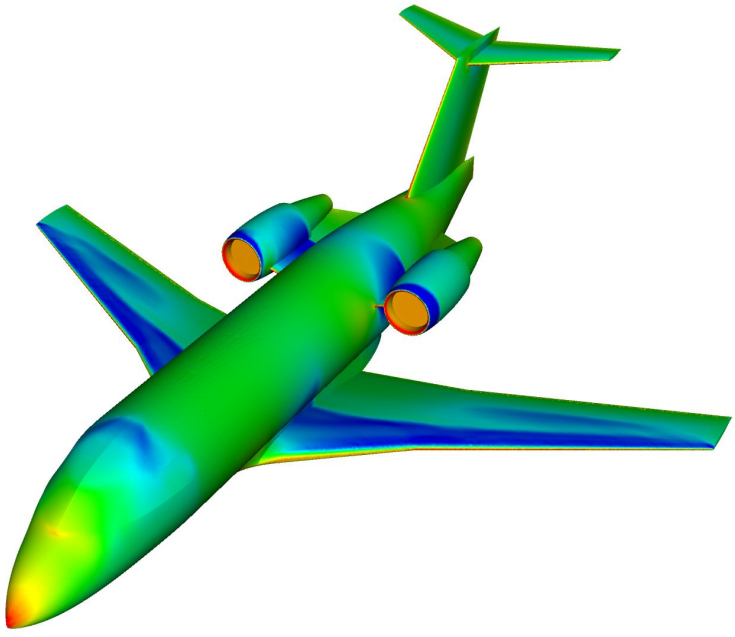

Division of Aeronautics, FFA
SE-172 90 STOCKHOLM

FOI – Swedish Defence Research Agency
Division of Aeronautics, FFA
SE-172 90 STOCKHOLM

FOI-R--1320--SE
September 2004
1650-1942

Scientific report

Stephen Conway

Implementation and Validation of an Engine Nacelle Boundary Condition in Edge 3.2

Division of Aeronautics, FFA
SE-172 90 STOCKHOLM

Contents

Abstract

The implementation of a boundary condition which enables the coupled computation of air flow in and out of engine nacelles is described and tested. The boundary condition is implemented into the hybrid solver Edge. User input is limited to specification of the pressure and temperature ratio at the nacelle exhaust. Two test cases are computed: a simple nacelle and a business jet fitted with two turbofan engines. Satisfactory results are obtained in both cases.

Nomenclature

A	Area
c	speed of sound
La	Laval number
$\dot{m}$	mass flow rate
M	Mach number
p	pressure
R	universal gas constant $(= 287 J/kgK)$
S	surface normal
T	temperature
U	velocity
ϵ	capture area
γ	ratio of specific heats
ρ	density
$\vec{()}$	vector value
$()'$	derivative
$()^*$	critical value
$()_i$	node value
$()_\infty$	free stream value
$()_0$	total state value
$()_{fan}$	value at fan face
$()_{est}$	estimated value
$()_{Ex}$	value at nacelle exhaust

1 Introduction

Proper integration of the propulsion system with the airframe of a modern aircraft is extremely important for the reduction of aerodynamic drag and to some extent noise. Determining optimum nacelle placement is a complex procedure and requires advanced computational and experimental studies. In order to carry out such computational studies it is important to model as accurately as possible the air flow around and into the engine nacelle. In this report the implementation and testing of a boundary condition which makes use of the air flowing in and out of the engine is described. The boundary condition requires input in the form of a pressure ratio and a temperature ratio at the engine exhaust. From this information a mass flow at the exhaust can then be computed and used to determine the flow entering the nacelle. The user also has the option of supplying the capture area as a boundary parameter or letting this be computed by the solver. The implementation is based on the method proposed by Rudnik [3] and described in [4].

2 Nacelle inlet computation

The calculation of the boundary values at the inlet to the nacelle is defined as follows. One should bare in mind that this boundary is in fact an outflow boundary condition with respect to the computational domain used in CFD calculations. At the nacelle inlet the air mass flux $\dot{m}$ is required as input. Knowing this and the fan area A_{fan}, a relationship can be derived for the capture area ϵ by calculating an equivalent mass flow in the free stream where A_∞ can be interpreted as the area of the streamtube formed slightly upstream of the nacelle. Note that in the case where ϵ is provided as a boundary condition the calculation of equations (1) and (2) are omitted in the calculation of the nacelle inlet.

$$\epsilon = \frac{A_\infty}{A_{fan}} \tag{1}$$

$$\epsilon = \frac{\dot{m}}{A_{fan} \cdot M_\infty \cdot \sqrt{\gamma p_\infty \rho_\infty}} \tag{2}$$

At this stage it is useful to introduce some isentropic relationships for air. We know that the Mach number is defined as:

$$M = \frac{U}{c} \tag{3}$$

and that for an ideal gas the following relationship for the speed of sound can be formulated:

$$c = \sqrt{\gamma RT} \tag{4}$$

From these relationships and the equation of state $(p = \rho RT)$ we can also formulate isentropic relationships for temperature, pressure and density as follows:

$$T = \frac{T_0}{1 + \frac{\gamma-1}{2} \cdot M^2} \tag{5}$$

$$p = p_0 \cdot \left(\frac{1}{1 + \frac{\gamma-1}{2} \cdot M^2} \right)^{\gamma/(\gamma-1)} \tag{6}$$

$$\rho = \rho_0 \cdot \left(\frac{1}{1 + \frac{\gamma-1}{2} \cdot M^2} \right)^{1/(\gamma-1)} \tag{7}$$

It is now helpful to introduce the *critical state* (or choked flow condition), denoted $()^*$, which is obtained when the Mach number, $M = 1$. This condition is used when describing the theoretical flow through converging-diverging ducts [2]. It can however be applied to the nacelle problem by defining the flow into the nacelle in terms of critical flow parameters as follows. By substituting $M = 1$ into equation (6) we obtain the critical pressure ratio:

$$\frac{p^*}{p_0} = \left(\frac{2}{\gamma + 1} \right)^{\gamma/(\gamma-1)} \tag{8}$$

Similarly we can obtain the critical temperature and density ratios as:

$$\frac{T^*}{T_0} = \frac{2}{\gamma+1} \tag{9}$$

$$\frac{\rho^*}{\rho} = \left(\frac{2}{\gamma+1}\right)^{1/(\gamma-1)} \tag{10}$$

We can also use the choked flow condition to define the ratio of local area, A, to critical area, A^*. Firstly consider the equation for conservation of mass for choked flow conditions:

$$\rho A U = \rho^* A^* U^* \tag{11}$$

then the critical area relation (A/A^*) can be defined as:

$$\frac{A}{A^*} = \left(\frac{\rho^*}{\rho}\right)\left(\frac{U^*}{U}\right) \tag{12}$$

And from equations (3) and (4) we have:

$$U^* = \sqrt{\gamma R T^*} \tag{13}$$

$$U = M \cdot \sqrt{\gamma R T} \tag{14}$$

Combining equations (13) and (14) and utilising the critical state relationship defined in equation (12), results in:

$$\frac{A}{A^*} = \frac{1}{M}\left(\frac{\rho^*}{\rho_0}\right)\left(\frac{\rho_0}{\rho}\right)\sqrt{\frac{(T^*/T_0)}{(T/T_0)}} \tag{15}$$

which when incorporating equations (5),(7), (9), (10) and (15) can be written as:

$$\frac{A}{A^*} = \frac{1}{M}\left[\frac{1+\frac{\gamma-1}{2}\cdot M^2}{1+\frac{\gamma-1}{2}}\right]^{\frac{(\gamma+1)}{2(\gamma-1)}} \tag{16}$$

At this stage it is helpful to introduce the Laval number which defines the ratio between the speed of the flow and the critical speed of sound and is defined as:

$$La = \frac{U_\infty}{c^*} \tag{17}$$

where:

$$c^* = \sqrt{\gamma R T^*} \tag{18}$$

is the critical speed of sound. Using the isentropic relationships once again, a free stream Laval number La_∞ can be defined. Using equations (3) and (18) the Laval number can be rewritten as:

$$La_\infty = \frac{M_\infty \sqrt{\gamma R T}}{\sqrt{\gamma R T^*}} \tag{19}$$

We can also write:

$$La_\infty = M_\infty \cdot \sqrt{\frac{T}{T^*}} = M \cdot \sqrt{\frac{T/T_0}{T^*/T_0}} \tag{20}$$

and using equations (5) and (9) a definition for the Laval number is obtained:

$$La_\infty = \sqrt{\frac{(\gamma+1)\cdot M_\infty^2}{(\gamma-1)\cdot M_\infty^2 + 2}} \tag{21}$$

The isentropic relationship for temperature can also be defined in terms of the Laval number as:

$$\frac{T}{T_0} = 1 - \frac{(\gamma-1)}{(\gamma+1)} \cdot La^2 \tag{22}$$

Using this relationship along with equations (3), (4), (17) and (18) it is also possible to define the Mach number in terms of the Laval number in the same manner as was done for equation (21). This results in the following relationship:

$$M_\infty = \sqrt{\frac{2La_\infty^2}{(\gamma+1) - (\gamma-1)\cdot La_\infty^2}} \tag{23}$$

Utilising the critical flow relation defined in equation (16) and the Laval number definition given in equation (21) a critical flow relation in terms of the Laval number can be defined as:

$$\frac{A^*}{A_\infty} = La_\infty \cdot \left[\frac{1 - \frac{\gamma-1}{\gamma+1}\cdot La_\infty^2}{1 - \frac{\gamma-1}{\gamma+1}}\right]^{\frac{1}{\gamma-1}} \tag{24}$$

An estimated Laval number La_{est} for the fan can be calculated by use of the critical flow area relation and the capture area as:

$$La_{est} = \epsilon \cdot \frac{A^*}{A_\infty} = \epsilon \cdot La_{fan} \cdot \left[\frac{1 - \frac{\gamma-1}{\gamma+1}\cdot La_{fan}^2}{1 - \frac{\gamma-1}{\gamma+1}}\right]^{\frac{1}{\gamma-1}} \tag{25}$$

This equation is solved iteratively where the value of La_{fan} at the previous iteration is used as the next estimate. The difference ΔA given by equation (26) is used to update the value of La_{fan}.

$$\Delta A = La_{est} - \epsilon \cdot \frac{A^*}{A_\infty} \tag{26}$$

The value of La_{fan} at the next iteration is given as:

$$La_{fan} = La_{fan} - (0.875 \cdot \frac{\Delta A}{La_{est}{}'}) \tag{27}$$

where 0.875 is a relaxation factor and $La_{est}{}'$ is the derivative of the estimated fan Laval number and is defined as:

$$La_{est}{}' = \frac{1}{\left(1-\frac{\gamma-1}{\gamma+1}\right)^{\frac{1}{\gamma-1}}} \cdot \left(1-\frac{\gamma-1}{\gamma+1}\cdot La_{\infty}^{2}\right)^{\frac{2-\gamma}{\gamma-1}} \cdot \left(1-\frac{\gamma-1}{\gamma+1}\cdot La_{\infty}^{2}\cdot\left(1+2\cdot\frac{1}{\gamma-1}\right)\right) \tag{28}$$

Convergence is reached when the difference ΔA is less than a predefined value, (1×10^{-15}). The value of La_{fan} obtained at the final iteration, along with the the free stream stagnation values can then be used to calculate the Mach number, speed of sound and pressure at the fan face. The stagnation free stream values are obtained from the following expressions for the speed of sound:

$$c_{0,\infty} = c_{\infty}\cdot\sqrt{1+\frac{\gamma-1}{2}\cdot M_{fan}^{2}} \tag{29}$$

and for the pressure:

$$p_{0,\infty} = p_{\infty}\cdot\left(1+\frac{\gamma-1}{2}\cdot M_{fan}^{2}\right)^{\frac{\gamma}{\gamma-1}} \tag{30}$$

And hence the values on the fan face are given by:

$$M_{fan} = \sqrt{\frac{2\cdot La_{fan}^{2}}{(\gamma+1)-(\gamma-1)\cdot La_{fan}^{2}}} \tag{31}$$

$$c_{fan} = \frac{c_{0,\infty}}{\sqrt{1+\frac{\gamma-1}{2}\cdot M_{fan}^{2}}} \tag{32}$$

$$p_{fan} = \frac{p_{0,\infty}}{\left(1+\frac{\gamma-1}{2}\cdot M_{fan}^{2}\right)^{\frac{\gamma}{\gamma-1}}} \tag{33}$$

The value of static pressure, p_{fan} is then specified at each node, i on the nacelle fan face. The other primitive variables are extrapolated at each node from the flowfield.

3 Nacelle exhaust computation

An inflow boundary condition is used to set the boundary values on the nacelle exhaust. Data in the form of a pressure ratio, $p_{0,Ex}/p_\infty$ and temperature ratio, $T_{0,Ex}/T_{0,\infty}$ are required. These values are given in the boundary condition file. From these ratios the stagnation values of temperature, pressure and density at the exhaust can be determined:

$$T_{0,Ex} = \left(\frac{T_{0,Ex}}{T_{0,\infty}}\right) \cdot T_{0,\infty} \tag{34}$$

$$p_{0,Ex} = \left(\frac{p_{0,Ex}}{p_\infty}\right) \cdot p_\infty \tag{35}$$

$$\rho_{0,Ex} = \frac{p_{0,Ex}}{R \cdot T_{0,Ex}} \tag{36}$$

Where $T_{0,\infty}$ is the global free stream stagnation temperature and p_∞ is the global static pressure. At the exhaust plane the pressure is extrapolated and the primitive variables are used to set the boundary condition as follows. With p known from the solution and with $T_{0,Ex}$ and $p_{0,Ex}$ obtained from equations (34) and (35) the Mach number can be determined using isentropic relationships:

$$M = \sqrt{\left[\left(\frac{p_{0,Ex}}{p}\right)^{\frac{\gamma-1}{\gamma}} - 1\right] \cdot \frac{2}{\gamma - 1}} \tag{37}$$

and the remaining primitive variables can be found by:

$$T = \frac{T_{0,Ex}}{\left(1 + \frac{\gamma-1}{2} \cdot M^2\right)} \tag{38}$$

$$\rho = \frac{p}{RT} \tag{39}$$

where the nodal values of the velocity can be computed as:

$$\vec{U}_i = \sqrt{\frac{2 \cdot \gamma}{\gamma - 1} \cdot \left(\frac{p_{0,Ex}}{\rho_{0,Ex}} - \frac{p_i}{\rho_i}\right)} \cdot \frac{\vec{S}_i}{|\vec{S}_i|} \tag{40}$$

where i represents the value at the boundary node. From this information and the cell surface normals $\vec{S}$, the mass flux across the exhaust plane can be determined by summing the flux across all boundary nodes:

$$\dot{m} = \sum_i \rho_i \cdot \vec{U}_i \cdot \vec{S}_i \tag{41}$$

Since this mass flux is used as input to the Nacelle inlet boundary condition it is essential that it is calculated prior to the nacelle inlet computation.

4 The Edge solver

Edge is a compressible Navier-Stokes solver for unstructured grids. The solver is based on an edge-based formulation for arbitrary elements and uses a node-centred finite volume technique to solve the governing equations. The governing equations are integrated explicitly towards steady state using Runge-Kutta time integration. A dual time stepping algorithm is also available for unsteady computations. Convergence acceleration is achieved using agglomeration multigrid and implicit residual smoothing. A number of turbulence models are available including a wide range of eddy viscosity type models and explicit algebraic Reynolds stress models (EARSM) [1].

5 Test cases

5.1 Case 1: Simple nacelle

As a first test of the nacelle boundary condition the external flow around a very simple nacelle geometry was computed. The nacelle consisted of a cylindrical section and a nozzle section. The area ratio between the inlet and outlet $(A_{in}/A_{out}$ was 4. The computational domain consisted of a $80m \times 50m \times 50m$ box $(l \times b \times h)$ and is shown in figure 1. Flow enters the domain along the x-direction at a speed of $50m/s$ $(M = 0.144)$ and a pressure of 1 bar. On the nacelle outlet boundary a pressure ratio $(p_{0,Ex}/p_{\infty})$ of 1.5 was set to simulate an energised flow through the engine. The temperature ratio, $(T_{0,Ex}/T_{0,\infty})$ was set to 1.0. An Euler calculation was performed on a single grid and convergence was obtained within 2000 iterations (figure 2).

Figure 1. Generic nacelle geometry

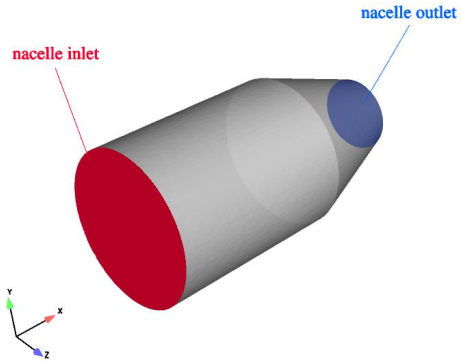

Figure 2. Convergence history

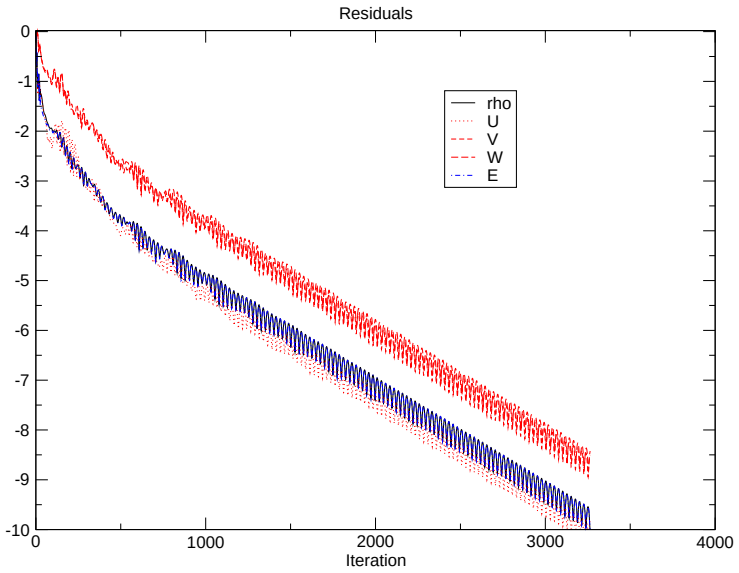

The boundary condition file used in this computation is included as an appendix in this report. A check of the mass balance (mass flow in = mass flow out of nacelle) showed agreement to within 1.7% in this case. The accelerated flow exiting the nacelle is shown in figure 3. In this figure streamlines are superimposed on the Mach number distribution at the centreline plane. The Mach number at the nacelle outlet is roughly 0.8. At the inlet the flow is accelerated from an ambient speed of $M = 0.144$ to roughly 0.22.

Figure 3. Mach distribution and streamlines

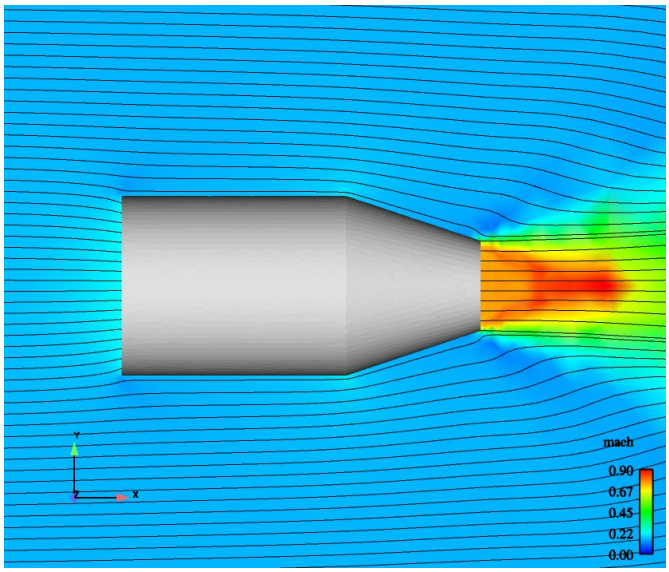

In figure 4 the pressure ratio $(p_{0,Ex}/p_\infty)$ is plotted over a cross-section of the nacelle exhaust. Near the outer edges of the exhaust some fluctuations are visible, these are possibly due to the weak formulation used in setting this type of boundary condition in Edge. The values obtained closer to the centre of the nacelle are more constant and have a value of 1.5 as expected. The positioning of the nacelle exhaust was found to have a substantial ef-

Figure 4. $p_{0,Ex}/p_\infty$ at a cross-section of the nacelle exhaust

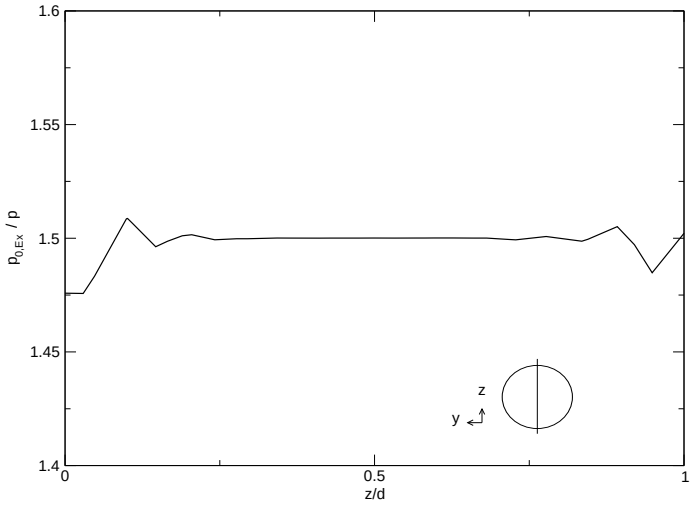

fect on the boundary values obtained. Two exhaust locations were considered as shown in figure 5. In the left hand figure, the exhaust boundary is

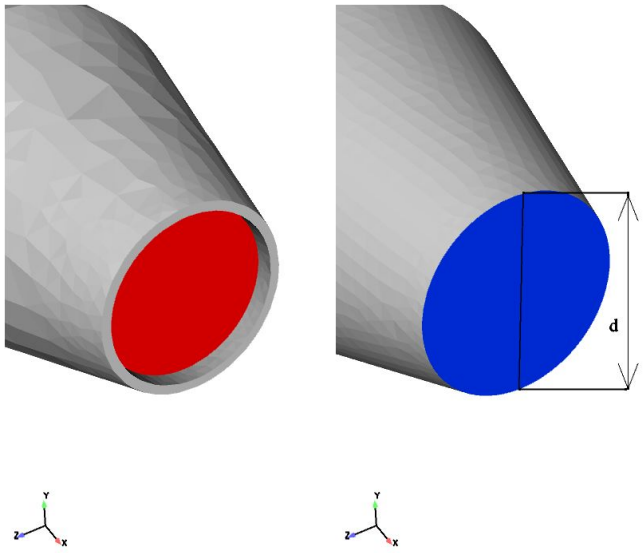

Figure 5. Two placements of the nacelle exhaust boundary, Left image: with base area. Right image: no base area

recessed and the outer wall has a base thickness of $0.1d$. In the right hand figure however the boundary is positioned such that the wall has no thickness. The influence of this positioning is shown in figure 6 where once again the pressure ratio is plotted over a cross-section of the nacelle exhaust. The fluctuations observed at the outer edge of the exhaust are much more pronounced in the case with no wall thickness, in some points almost 40% of the total pressure. This figure also includes results obtained using a Mach number extrapolation at the boundary. Here one can see that the pressure extrapolation method gives a reduction in the fluctuations. In this case however the greatest reduction in fluctuations is obtained by recessing the exhaust boundary slightly.

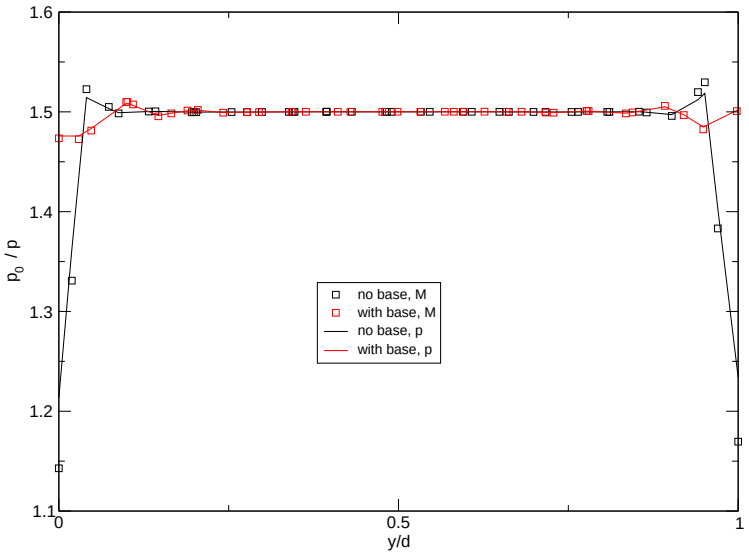

Figure 6. Two exhausts and two method of extrapolation: p = pressure extrapolation, M = Mach extrapolation

5.2 Case 2: Bombardier Challenger 604

A Bombardier Challenger 604 business jet was used as a second test case for validating the nacelle boundary conditions. This aircraft is fitted with two General Electric CF34-3B turbofan engines [5]. The computational mesh for this geometry was obtained from SAAB and consists of roughly 1 million tetrahedrons. A free stream Mach number of 0.8, equivalent to the cruise speed of the jet, and an angle of attack of 1.5° were set. For the nacelle exhaust the pressure ratio was set to 1.75 and the temperature ratio was set to 1.0. At the nacelle inlet an area ratio ϵ of 0.75 was given. A weak characteristic boundary condition was used in the farfield and on the by-pass outlets of the engines. The Euler equations were solved and three levels of multigrid were used. Convergence was obtained after roughly 600 iterations on the finest grid as shown in figure 7. The Tau code (version

Figure 7. Convergence history for Edge computation

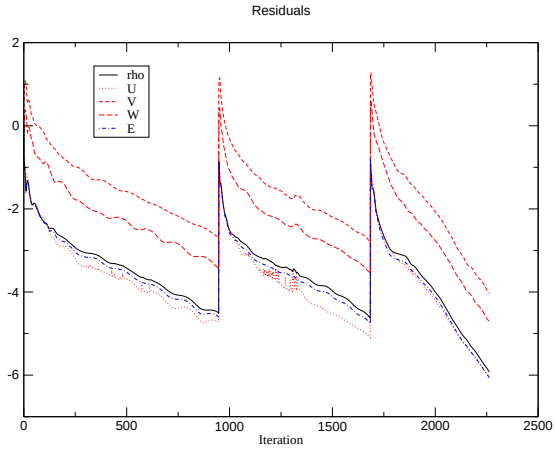

2002.1.1) [4] was used to provide a reference solution. Since the boundary condition has been tried and tested in this solver a comparison between the Tau and Edge solution should provide enough information to verify the implementation in Edge.

To fulfill mass conservation the mass of air flowing into and out of the engine nacelle should be equal. From table 1 it is clear that in both cases mass is conserved since for this particular nacelle:

$$m_{inlet} = m_{bypass} + m_{outlet} \tag{42}$$

where m_{inlet} is the mass flowing into the engine nacelle, m_{outlet} is the mass flow from the nacelle exhaust and m_{bypass} is the mass flow through the bypass region of the nacelle.

Table 1. Components of mass flow through the engine nacelle

Mass flow $[kg/s]$	Edge	Tau
Nacelle Inlet	379.7	379.0
Nacelle Bypass	234.2	232.2
Nacelle Outlet	145.5	146.8

Note that there is a difference of only 0.2% in the overall mass flow when comparing the Edge and Tau solutions. It is also important to make sure that the aerodynamic results given by the solvers are in agreement. By comparing the pressure distribution on one of the wings we can see that the solutions compare very well. Figure 8 shows Cp at 20, 40, 60 and 80% span.

Figure 8. Cp comparison at 4 positions

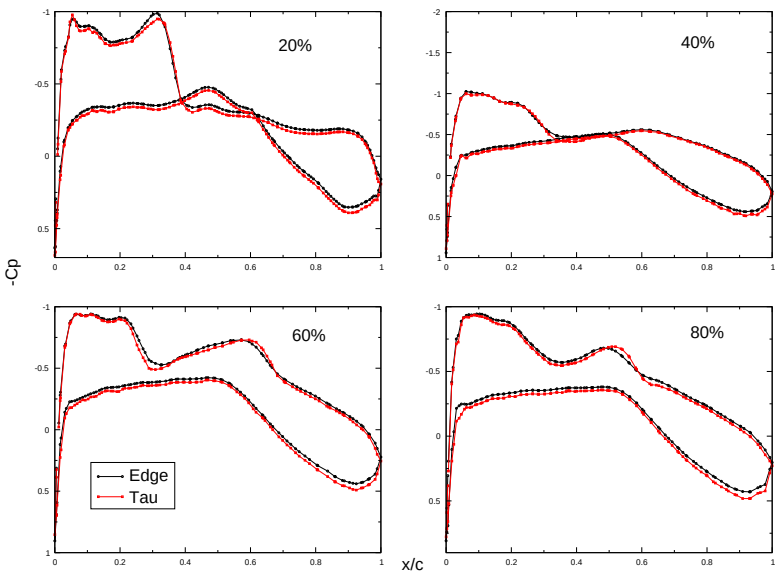

A comparison in the Cp distribution on the nacelle inlet surface is shown in figure 9. Once again it is clear that the solutions compare very well.

Figure 9. Cp at the nacelle inlet

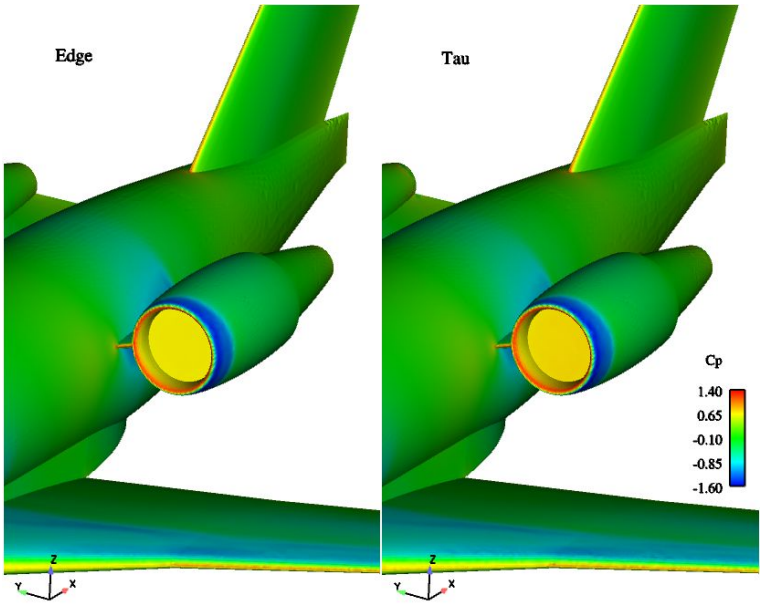

The Mach number distribution across the centreline of the nacelle inlet is shown in figure 10. Almost identical results are obtained from the solvers.

Figure 10. Mach distribution across centreline of nacelle inlet

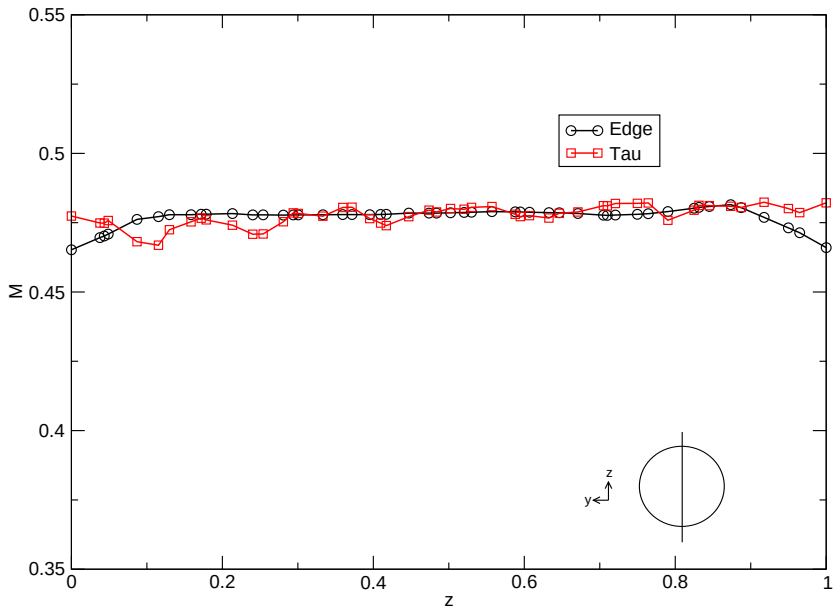

If we now consider the flow exiting the nacelle and plot the ratio of total pressure $p_{0,Ex}/p$ across the centreline of the exhaust plane we see that near the centre of the nacelle exhaust very similar pressures are obtained and the expected value of 1.75 is obtained in both the Edge and Tau computation. However close to the walls of the nacelle the results differ, and a large drop in the total pressure is visible in the Edge result. This is also seen to a lesser extent in the Tau result.

Figure 11. $p_{0,Ex}/p$ at the nacelle exhaust

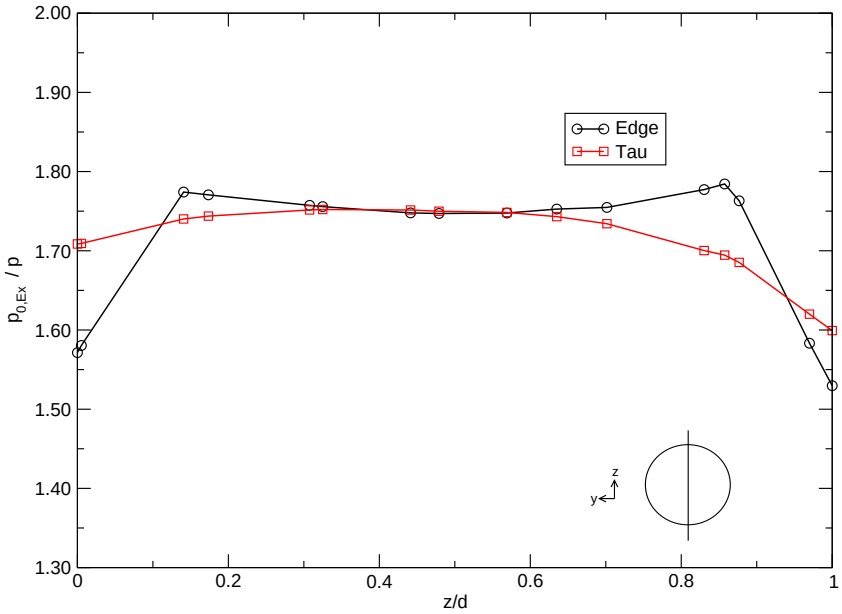

As discussed previously the reason for this occurring in Edge can be due to the combined effect of the placement of the nacelle boundary and the treatment of this type of boundary condition in the solver. Figure 12 depicts the specific mass flow ($\dot{m} = \rho \cdot \vec{U}$) across the same section. Once again we notice a drop at the outer edge of the boundary. Close to the centre however the mass flow is very similar for each of the solvers.

Figure 12. Specific mass flow at the nacelle exhaust

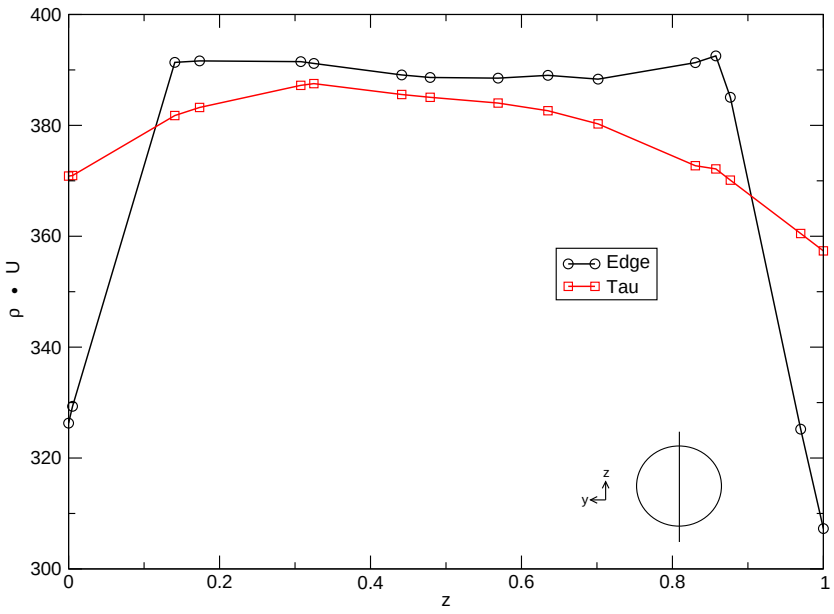

6 Conclusion

A new boundary condition which enables the coupled computation of engine nacelle inlets and exhausts has been implemented and tested in the Edge solver. Two test cases have been computed and encouraging results have been obtained. The boundary condition is simple for the user to specify, requiring only the input of a pressure and temperature ratio at the nacelle exhaust. For the Euler calculations carried out here it was found that the choice of extrapolation method combined with the weak formulation of the boundary condition at the nacelle exhaust resulted in fluctuations in the primitive variables close to the outer edge of the nacelle exhaust. The positioning of the nacelle exhaust was also found to influence the solution. By recessing the exhaust boundary into the geometry of the simple nacelle studied in test case 1 the level of fluctuations in total pressure were greatly reduced. A comparison using the Tau solver with the same nacelle boundary condition gave very similar results to those obtained in Edge.

References

[1] Eliasson, P. Edge, A Navier-Stokes Solver for Unstructured Grids. *FOI-R–0298–SE,* 2001. `www.Edge.foi.se`

[2] Munson, B.R., Young, D.F. & Okiishi, T.H. Fundamentals of Fluid Mechanics, *John Wiley & Sons*, 1990.

[3] Rudnik, R. Erweiterung eines dreidimensionalen Euler-Verfahrens zur Berechnung des Strömungfeldes um Nebenstromtriebwerke mit Fan- und Kernstrahl. *DLR-FB 91-13*, 1991.

[4] Tau technical Documentation version 2002.1.0. DLR.

[5] `www.bh.com/companions/034074152X/appendices/data-b/table-2/default.htm` also `www.bombardier.com`

Appendix A

Sample Boundary Condition File

This is the boundary condition file for the simple nozzle computation. The data for the nacelle boundary condition is found under `'nacelle exhaust'` and `'nacelle inlet'`.

```
boundary_data    N      0         0    6
  boundary         NB     0         0    3
    b_name           L      1         1    0
 'BC1_on_FARFIELD                                                        '
    b_class          L      1         1    0
 'external                                                               '
    b_type           L      1         1    0
 'weak characteristic                                                    '
  boundary         NB     0         0    3
    b_name           L      1         1    0
 'BC1_on_INLET                                                           '
    b_class          L      1         1    0
 'external                                                               '
    b_type           L      1         1    0
 'weak characteristic                                                    '
  boundary         NB     0         0    5
    b_name           L      1         1    0
 'BC1_on_NACELLE_OUT                                                     '
    b_class          L      1         1    0
 'external                                                               '
    b_type           L      1         1    0
 'nacelle exhaust                                                        '
    pres_ratio       R      1         1    0
 1.50000000
    temp_ratio       R      1         1    0
 1.00000000
  boundary         NB     0         0    3
    b_name           L      1         1    0
 'BC1_on_CYL                                                             '
    b_class          L      1         1    0
 'wall                                                                   '
    b_type           L      1         1    0
 'weak euler                                                             '
  boundary         NB     0         0    3
    b_name           L      1         1    0
 'BC1_on_OUTLET                                                          '
    b_class          L      1         1    0
 'external                                                               '
    b_type           L      1         1    0
 'weak characteristic                                                    '
  boundary         NB     0         0    4
    b_name           L      1         1    0
 'BC1_on_NACELLE_IN                                                      '
    b_class          L      1         1    0
 'external                                                               '
    b_type           L      1         1    0
 'nacelle inlet                                                          '
    eps_fan          R      1         1    0
 0.00000000E+00
```

Issuing organisation
FOI – Swedish Defence Research Agency
Division of Aeronautics, FFA
SE-172 90 STOCKHOLM

Report number, ISRN
FOI-R--1320--SE

Report type
Scientific report

Month year
September 2004

Project number
A830021

Customers code
3. Aeronautical Research

Research area code
7. Vehicles

Sub area code
73. Aeronautical Research

Author(s)
Stephen Conway

Project manager
Peter Eliasson

Approved by
Torsten Berglind
Head, Computational Aerodynamics Department

Scientifically and technically responsible
Peter Eliasson

Report title
Implementation and Validation of an Engine Nacelle Boundary Condition in Edge 3.2

Abstract
The implementation of a boundary condition which enables the coupled computation of air flow in and out of engine nacelles is described and tested. The boundary condition is implemented into the hybrid solver Edge. User input is limited to specification of the pressure and temperature ratio at the nacelle exhaust. Two test cases are computed: a simple nacelle and a business jet fitted with two turbofan engines. Satisfactory results are obtained in both cases.

Keywords
CFD, Edge, Nacelle, Boundary conditions

Further bibliographic information

ISSN
1650-1942

Pages
35

Language
English

Price
Acc. to price list

Security classification
Unclassified

Utgivare	Rapportnummer, ISRN	Klassificering
Totalförsvarets Forskningsinstitut – FOI Avdelningen för Flygteknik, FFA SE-172 90 STOCKHOLM	FOI-R--1320--SE	Vetenskaplig rapport
	Månad år September 2004	Projektnummer A830021
	Verksamhetsgren 3. Flygteknisk forskning	
	Forskningsområde 7. Farkoster	
	Delområde 73. Flygteknisk forskning	
Författare Stephen Conway	Projektledare Peter Eliasson	
	Godkänd av Torsten Berglind Chef, Institutionen för beräkningsaerodynamik	
	Tekniskt och/eller vetenskapligt ansvarig Peter Eliasson	
Rapporttitel Validering av ett Motorgondol Randvillkor i Edge 3.2		
Sammanfattning Ett randvillkor som gör det möjligt att genomföra kopplade beräkningar av luftströmningen in och ut från en motorgondol har implementerats och validerats i strömningslösaren Edge. Användaren behöver bara specificera ett tryck och temperatur förhållande vid utloppet från gondolen. Två valideringsfall har räknats: en enkel motorgondol geometri och ett tvåmotorigt turbofläkt affärsjet.		
Nyckelord CFD, Edge, Motorgondol, Randvillkor		
Övriga bibliografiska uppgifter		
ISSN 1650-1942	Antal sidor 35	Språk Engelska
Distribution enligt missiv	Pris Enligt prislista	
	Sekretess Öppen	